

Two and more interacting particles at a metal-insulator transition

Andrzej Eilmes¹, Rudolf A. Römer², Cosima Schuster³, and Michael Schreiber²

¹Department of Computational Methods in Chemistry,

Jagiellonian University, Ingardena 3, 30-060 Kraków, Poland

²Institut für Physik, Technische Universität, D-09107 Chemnitz, Germany

³Institut für Physik, Universität Augsburg, D-86135 Augsburg, Germany

(*Revision* : 1.35, compiled February 7, 2020)

We study the influence of many-particle interactions on a metal-insulator transition. First, we consider the two-interacting-particle problem for onsite interacting particles on a one-dimensional quasiperiodic chain, the so-called Aubry-André model. We show numerically by the decimation method and finite-size scaling that the interaction does not modify the critical parameters such as the transition point and the localization-length exponent. Second, we employ the density-matrix renormalization scheme to investigate the finite density situation. We map out the entire phase diagram and find that there is a Peierls-like transition into a metallic state for attractive interactions. Our results also show agreement with a recent analytic renormalization group approach.

71.30.+h, 71.27.+a

I. INTRODUCTION

The metal-insulator transition (MIT) in disordered electronic systems has been the subject of intense research activities over the last two decades and still continues to attract much attention. For free electrons in disordered systems [1] the scaling hypothesis of localization [2] can successfully predict many of the universal features of the MIT. However, the influence of many-particle interactions on the MIT is not equally well understood [3] and recent investigations of an apparent MIT in two-dimensional (2D) systems even question the main assumptions of the scaling hypothesis [4–9]. A simple theoretical approach to the interplay of interactions and disorder is based on the two-interacting-particles (TIP) problem in 1D random [10–12] or quasiperiodic potentials [13,14]. Furthermore, numerical results for spinless fermions at finite particle density have given additional insight [15,16]. In general, these investigations have shown that changes in the wave function interferences due to many-particle interactions [17,18] can lead to a rather large enhancement of the localization lengths in 1D and 2D [16,19,20].

The standard approach for computing localization lengths in disordered, non-interacting systems is the transfer-matrix method [21]. It has been used for investigations of the enhancement of the TIP localization length in a 1D random potential [12,22] where there is no MIT as all wave functions are always localized. Other numerical approaches to the TIP problem have been based on the time evolution of wave packets [10,23], exact diagonalization [24] or Green function approaches [19,25,26].

In the single-particle case, the 1D quasiperiodic Aubry-André model is known rigorously to exhibit an MIT for all states in the spectrum as a function of the quasiperiodic potential strength μ [27]. The ground state wave function is extended for $\mu < 1$ and localized for $\mu > 1$.

The system at $\mu_c = 1$ is critical: there the wave functions decrease algebraically, not exponentially as in the localized case. Recently, we examined this model for TIP by means of the transfer-matrix method together with a careful finite-size-scaling analysis [14] following earlier analytical work of Refs. [28,29]. We showed that the model for TIP exhibits an MIT as a function of μ at $\mu_c = 1$ as in the single-particle case. Our finite-size-scaling results for onsite (Hubbard) interaction suggest that the critical behavior, i.e., the value for the critical exponent ν of the correlation length, is also not affected by the interaction [14]. However, it has been demonstrated [12,19] that a transfer-matrix-method approach applied to the TIP problem without finite-size scaling leads to unreliable localization lengths, i.e., it systematically overestimates the TIP localization length λ_2 in finite-sized samples in the case of vanishing interaction ($U = 0$). In addition, simple extrapolations to infinite sample size [22,12] may lead to an underestimation of λ_2 [30]. An alternative approach, which does not suffer from the above problem, is based on the decimation method and has also been applied recently to TIP in a 1D random potential [19]. This encouraged us to reexamine the localization lengths for TIP in 1D quasiperiodic potentials with Hubbard interaction with the decimation method. As we shall show in the following, we find that the general conclusions of Ref. [14] remain valid, i.e., the MIT is not affected by the interaction.

As an independent extension of these low-density results, Chaves and Satija [31] have studied a model of nearest-neighbor interacting spinless fermions [32–34] at finite particle density in the same quasiperiodic potential by means of Lanczos diagonalization for small systems up to chain size $M = 13$. They find evidence for a critical region in which the behavior of the charge stiffness [35–37] is different from its behavior in the metallic and localized regimes. In order to reach much larger system sizes for

interacting systems, we employ the numerical density-matrix renormalization group (DMRG) [38] which has been shown to be very useful [39]. In particular, the ground state properties of interacting many-particle systems in 1D can be obtained very accurately [40,41]. In the present paper, we shall study the quasiperiodic model of Ref. [31] at various densities and interaction strengths V by DMRG and compare our results to the TIP data.

Our results show that in the low-density TIP case, the critical properties of the single-particle transition at $\mu_c = 1$ are not altered within the accuracy of our calculation. One-parameter scaling is obeyed for onsite interaction strengths up to $U = 10$. For the interacting many-body system in a quasiperiodic potential we recover the single-particle transition at $\mu_c = 1$, provided we consider densities like $\rho = 1/2$ which are incommensurate compared to the wave vector of the quasiperiodic potential — an irrational multiple of π . On the other hand, for commensurate densities, we find that the system can be completely localized even for $\mu \ll 1$. Whereas for repulsive interactions the ground state remains localized, we find a region of extended states for attractive interaction due to a Peierls resonance between electronic and quasiperiodic potential degrees of freedom. The behavior may be described by a weak-coupling renormalization group (RG) treatment [42].

The paper is organized as follows. In section II we describe the Hamiltonian of our TIP system and explain how to obtain the TIP localization lengths via decimation method. In section III, we comment on the particular finite-size-scaling method employed and present the estimated critical parameters. The finite-density many-body system is introduced in section IV and results are presented in section V. We summarize and conclude in section VI.

II. THE TIP SYSTEM AND THE NUMERICAL APPROACH

The Hamiltonian for TIP in the 1D quasiperiodic potential of the Aubry-André model is given as

$$\mathbf{H} = \sum_{n,m} |n, m\rangle \langle n+1, m| + |n, m\rangle \langle n, m+1| + \text{h. c.} + |n, m\rangle [\mu_n + \mu_m + U(n, m)] \langle n, m| . \quad (1)$$

Here $\mu_m \equiv 2\mu \cos(\alpha m + \beta)$ is the quasiperiodic potential of strength μ with $\alpha/2\pi$ being an irrational number. β is an arbitrary phase shift and we choose $\alpha/2\pi = (\sqrt{5} - 1)/2$, i.e., the inverse of the golden mean. This value of $\alpha/2\pi$ may be approximated by the ratio of successive Fibonacci numbers — $F_n = F_{n-2} + F_{n-1} = 0, 1, 2, 3, 5, 8, 13, \dots$ — as is customary in the context of quasiperiodic systems [43]. The Hubbard onsite interaction matrix $U(n, m)$ is diagonal, i.e., $U(n, m) = U\delta_{nm}$.

The indices n and m correspond to the positions of each particle on a chain of length M . Now we use the decimation method [19,44] to construct an effective Hamiltonian for the diagonal of the $M \times M$ lattice along which the cigar-shaped TIP wave function has its largest extent [24,30]. The quantity of interest is the TIP localization length λ_2 defined by the TIP Green function $\mathbf{G}_2(E)$ [25]:

$$\frac{1}{\lambda_2} = -\frac{1}{|M-1|} \ln |\langle 1, 1 | \mathbf{G}_2 | M, M \rangle| . \quad (2)$$

For TIP in 1D and 2D random potentials, this approach has led to high precision results supporting the proposed increase of the TIP localization lengths due to the repulsive interaction [19,20]. We remark that similar data have also been obtained for nearest-neighbor [25] and long-ranged interactions [23].

The correlation length ξ_∞ for the infinite system may be obtained from the localization lengths $\lambda(M)$ for finite system sizes by the using one-parameter scaling hypothesis $\Lambda_M = f(M/\xi_\infty)$ [45] for the reduced localization lengths $\Lambda_M = \lambda(M)/M$. The MIT is characterized by a divergent correlation length $\xi_\infty(\mu) \propto |\mu - \mu_c|^{-\nu}$ [1]. In order to reliably extract the critical parameters from the calculated values of $\lambda_2(M)$ one may apply a finite-size-scaling procedure [21] that numerically minimizes deviations of the data from the common scaling curve f . The critical exponent ν can then be extracted by fitting the ξ_∞ obtained from finite-size scaling. This method was used previously [14] for finding the critical parameters of the present model.

Higher accuracy can be achieved by a method applied recently [46,47] to the MIT in the Anderson model of localization. We construct a family of fit functions which include corrections to scaling such as (i) nonlinearities of the dependence of the scaling variable on the quasiperiodic potential strength and (ii) an irrelevant scaling variable which accounts for a shift of the crossing point of the $\Lambda_M(\mu)$ curves as a function of μ , i.e.,

$$\Lambda_M = \tilde{f}(\chi_r M^{1/\nu}, \chi_i M^y) . \quad (3)$$

where χ_r and χ_i are the relevant and irrelevant scaling variables, respectively. \tilde{f} is then Taylor expanded up to order n_i in terms of the second argument

$$\Lambda_M = \sum_{n=0}^{n_i} \chi_i^n M^{ny} \tilde{f}_n(\chi_r M^{1/\nu}) , \quad (4)$$

and each \tilde{f}_n is Taylor expanded up to order n_r :

$$\tilde{f}_n = \sum_{i=0}^{n_r} a_{ni} \chi_r^i M^{i/\nu} . \quad (5)$$

Nonlinearities are taken into account by expanding χ_r and χ_i in terms of $u = (\mu_c - \mu)/\mu_c$ up to order m_r and m_i , respectively,

$$\chi_r(u) = \sum_{n=1}^{m_r} b_n u^n, \quad \chi_i(u) = \sum_{n=0}^{m_i} c_n u^n \quad , \quad (6)$$

with $b_1 = c_0 = 1$. The fit function is being adjusted to the data by choosing the orders n_i, n_r, m_r, m_i up to which the expansions are carried out. Of course, the orders have to be taken not too large to keep the number of fit parameters a_{ni} , b_n , and c_n reasonably small.

III. NUMERICAL RESULTS FOR TIP

We have calculated λ_2 at energy $E = 0$ for 20 values of the Hubbard interaction, i.e., $U = 0$ (the non-interacting single-particle case), $0.1, \dots, 0.9, 1, 2, \dots, 10$ for 6 system sizes $M = 13, 21, 34, 55, 89, 144$. For $U = 0$ and 1 , we also have data for $M = 233$ and 377 . The quasiperiodic potential strengths μ were chosen close to the single-particle transition at $\mu_c \approx 1$ and ranged typically from 0.95 to 1.05 . As in Ref. [14] we averaged the results over different randomly chosen phase shifts β in order to reduce the fluctuations. The number of β values used in this averaging ranged from 5000 for $M = 13$ to 1000 for $M = 377$. In order to perform the non-linear fit necessary for the finite-size-scaling procedure as outlined in section II, we used the Levenberg-Marquardt method [47,48]. As the decimation method data — like the transfer-matrix-method results [14] — are still rather noisy we have to suitably limit the ranges of the quasiperiodic potential strength μ and/or the system sizes M used for fitting the data.

For $U = 0$ and 1 , which were examined by the transfer-matrix method in detail [14], the best fit was obtained for $n_r = 3$, $n_i = 2$, $m_r = 2$ and $m_i = 1$. For $U = 0$ we used the data for μ ranging from 0.96 to 1.01 and $M = 55, 89, 144, 233$, and 377 ; for $U = 1$ we used all system sizes $M = 13, \dots, 377$ and $0.97 \leq \mu \leq 1.05$. Figs. 1 and 2 show the resulting TIP localization lengths for $U = 0$ and 1 . Also shown are the fits of the finite-size-scaling curves to the data as given by Eq. (3) for $U = 0$ and 1 , respectively. We find that for both U values, there is an apparent transition close to $\mu_c = 1$. For the case $U = 0$, we also observe a systematic shift of the crossing point with increasing system sizes necessitating the inclusion of an irrelevant scaling variable as discussed in section II. The transition point is not so clearly distinguished for $U = 1$, albeit the different behavior for $\mu \lesssim 1$ and $\mu \gtrsim 1$, namely the increase and decrease, respectively, of Λ_M with increasing M , is clearly seen.

The corresponding plots of the scaling curves are displayed in the insets of Figs. 1 and 2. The scaling curves are much better than reported previously [14] for the transfer-matrix-method data. The critical parameters can consequently be estimated to be $\mu_c = 0.989 \pm 0.001$, $\nu = 1.00 \pm 0.15$ for $U = 0$ and $\mu_c = 0.997 \pm 0.001$,

$\nu = 1.19 \pm 0.16$ for $U = 1$. The irrelevant scaling exponents are close to $y = 1.8 \pm 0.2$ and $y = 0.15 \pm 0.1$ for $U = 0$ and 1 , respectively. Note that the quoted errors correspond to the standard deviations estimated from the non-linear fit procedure. In this way the accuracy is significantly overestimated. Since it is apriori not clear, which values n_i, n_r, m_r, m_i to use, we estimate the true errors from a comparison of various fits with different n_i, n_r, m_r, m_i . Even in the case of extremely high precision data close to the MIT in the Anderson model of localization, this has been shown [47] to increase the error by one order of magnitude. Therefore we conclude that the interaction strength U for TIP does not influence the MIT in the quasiperiodic potential within the accuracy of the present calculation.

Further results for larger U values are collected in Table I. The expansion orders n_i, n_r, m_r, m_i , the system sizes and ranges of the quasiperiodic potential strength have been chosen in order to minimize the χ^2 statistics and to get the most convincing scaling fit. Fig. 3 shows the values of the critical quasiperiodic potential strength μ_c and the critical exponent ν . For almost all cases the critical quasiperiodic potential strength μ_c remains close to 1 , the only exceptions are $U = 0$ and 0.1 , when $\mu_c = 0.99$ and 0.98 , respectively. However, since we know that the transition in the single-particle case is exactly at $\mu_c = 1$ [27], this observation can be used to estimate the true error of the estimate for μ_c . Thus comparing with the μ_c estimates for $U \neq 0$, we find that the errors calculated within the non-linear fitting procedure are significantly underestimated as discussed above. We therefore conclude that there is no change of the critical quasiperiodic potential strength within $0 \leq U \leq 10$ within the accuracy of our calculation. The same argument leads to the conclusion that within the error bars the critical exponent ν does not change with the Hubbard interaction strength and is close to 1 . This is an agreement with the previous results obtained by the transfer-matrix method and finite-size scaling [14]. We stress that the critical exponents can be obtained with much less accuracy than the transition point μ_c as shown in Table I.

IV. THE NEAREST-NEIGHBOR HAMILTONIAN AT FINITE DENSITY AND THE DMRG

Let us now consider N interacting spinless fermions on a 1D ring of circumference M in the Aubry-André potential such that

$$H = -t \sum_m (c_{m+1}^\dagger c_m + \text{h. c.}) + V \sum_m n_{m+1} n_m + 2\mu \sum_m n_m \cos(\alpha m + \beta). \quad (7)$$

The operators c_m^\dagger , c_m , and n_m denote as usual Fermi creation, annihilation and number operators; α , β and μ

are defined as in the previous sections. In addition, we set $t = 1$. The particle density is $\rho = N/M$. Again, we choose $M = F_n$ and $\alpha/(2\pi) = F_{n-1}/F_n$ in order to retain the periodicity of the quasiperiodic potential on the ring. The model has been studied extensively in two limits, namely, $V = 0$ and $\mu = 0$. The first case corresponds of course to the non-interacting model discussed briefly in section I. In the second case, the model can be mapped onto the anisotropic Heisenberg (XXZ) model for which a closed Bethe-ansatz solution exists [32–34]. It shows three distinct phases at zero temperature. For half filling ($\rho = 1/2$) and strong repulsive interaction ($V > 2$) the system is a charge-density-wave insulator. For weak and intermediate interaction strength and away from half filling it is a metal and can be described as a Luttinger liquid with linear energy dispersion and gapless excitations [35,49]. The metal, at least, is separated for all fillings by a first-order transition at $V = -2$ from an insulator where the fermions form clusters (phase-separated state), corresponding to the ferromagnetic state of the spin model [34].

In a previous analysis [31] of the interacting quasiperiodic model (7), a large enhancement of the Drude weight D (or Kohn stiffness) [50] and the superconducting fluctuations in the ground state was found near the first-order transition at $V \approx -2$ using exact Lanczos diagonalization. However, the system sizes attainable by the diagonalization were restricted to $M \leq 13$. Using the DMRG, it is possible to extend the tractable system lengths to about $M \approx 100 - 200$. We use the finite lattice algorithm for non-reflection-symmetric models as described in [52]. In our simulations we perform five lattice sweeps and keep 300 (small systems) to 500 (larger systems, $M = 89$ and 144) states per block. As our observable of the phase transition we choose the phase sensitivity

$$M\Delta E = M(-1)^N [E(0) - E(\pi)] \quad (8)$$

of the ground state [41], which is connected to D in the clean case (Luttinger phase) and equal to $\pi^2 D$ for non-interacting fermions. Here $E(\Phi)$ measures the reaction of the system due to a twist in the boundary condition, $c_{M+1} = \exp(i\Phi)c_1$ [35,36]. The prefactor $(-1)^N$ cancels the odd-even effects [51]. In addition, it is believed that the phase sensitivity matches the character of the wave function. It does not depend on system size if the wave function is extended, e.g., for $\mu = 0$, and it decreases exponentially for large systems if the wave function is localized [41]. As argued in Ref. [31] this can be transferred to the critical case. Therefore, we suppose that the phase sensitivity decreases algebraically with increasing system size, if the wave function is critical. Thus, we have to compare at the very least three different chain lengths in order to characterize the length dependence of the wave function.

In order to do so reliably, we should compute $M\Delta E$ for these different chain lengths at the same particle density

ρ . However, incommensurate — compared to the wave vector of the quasiperiodic potential — particle densities are difficult to treat if we use $M = F_n$ as in the previous sections. For example, half filling can only be realized for even system size, i.e., for $M = 34, 144$, and 610, one-third filling for $M = 21, 144, 987$. In principle, such large system sizes $M > 500$ can be treated within the DMRG [52], but the required accuracy (10^{-6}) is very hard to obtain for periodic boundary conditions. In addition, if the phase sensitivity decreases with system size, there is no possibility to decide whether the decrease is algebraic or exponential because the obtained value of $M\Delta E$ for such large system sizes is already zero within the computational accuracy. For example, let us briefly comment on the non-interacting case with $\rho = 1/2$. Using a standard diagonalization routine, we investigate the system sizes $M = 34, 144$, and 610. $M = 8$ is excluded because $\alpha/(2\pi) = 5/8 = 0.625$ differs too much from the true value $(\sqrt{5} - 1)/2 \approx 0.618$. As shown in Fig. 4, the phase sensitivity at $V = 0$ is clearly different in the localized, critical and extended regimes. Thus, for a system of free fermions at finite density, we reproduce the expected transition at $\mu_c = 1$ in agreement with Refs. [14,31]. Although similar plots can be made for attractive and repulsive interactions at $\rho = 1/2$ as also shown in Fig. 4, unfortunately, with only two system sizes available ($M = 34$ and 144) for the interacting system, further conclusions appear rather speculative. We remark that our attempts to simulate incommensurate densities like $\rho = 1/4, 1/3, 1/2$ at fixed $\alpha/2\pi = (\sqrt{5} - 1)/2$ for system lengths $M \neq F_n$ by averaging over the β 's failed. No significant length dependence of the phase sensitivity could be detected using these densities and system lengths.

V. NUMERICAL RESULTS FOR FINITE PARTICLE DENSITY

For the reasons outlined in the last section, we shall study the behavior at the commensurate densities $\rho_i \approx \lim_{n \rightarrow \infty} F_{n-i}/F_n \approx 0.618, 0.382, 0.236$, and 0.146 corresponding to $i = 1, \dots, 4$ in the following, where $\alpha = 2\pi\rho_1$. We first note that the case of ρ_1 is identical to ρ_2 due to the particle-hole symmetry in Eq. (7). Averaging over different β values was not necessary since the computed ground-state energy of the finite-density Hamiltonian does not depend on β for $M = F_n$, i.e., if we include a complete period of the potential on the ring.

In Fig. 5, we summarize our results by showing two phase diagrams of model (7) for varying quasiperiodic potential strength μ and nearest-neighbor interaction V . They were obtained by studying the system size behavior of $M\Delta E$ up to $M = 144$ for $\rho_3 = 0.236$ and $\rho_4 = 0.146$. As an example how well the transition point is defined numerically consider Fig. 6. The localized regime extends further on to larger interactions, $-1.4 \lesssim V < \infty$, for ρ_3

and $\mu > 0$ as well as for ρ_4 and $\mu \gtrsim 0.1$. This part of the phase diagram is not shown, because it has no additional structure. Thus, in the repulsive regime ($V > 0$), we find that the ground state is localized for $\mu > 0$. This is in agreement with previous studies for disordered and periodically disturbed systems [15,41]. We emphasize that an increase of the localization lengths as predicted by the arguments for TIP [10] in sections II and III is most likely too small [16] to be detected by the present accuracy.

For attractive interactions, the situation is more interesting. For all densities ρ_i and $\mu \rightarrow 0$, the system shows *Peierls-like* behavior, i.e., a transition from insulating to metallic phase at $V \approx -1.4$. An equivalent critical behavior is found in the periodic hopping model, where the site-dependent hopping amplitude is given by $t_m = 1 - \delta \cos qm$ instead of t . In this model, which is usually called the Peierls [53] or Su-Schrieffer-Heeger model [54], the MIT occurs at $V = -\sqrt{2}$ and $\delta \rightarrow 0$, if filling factor ρ and wave vector q of the periodic hopping are commensurate, i.e., $\rho = q/(2\pi)$ or $q = 2k_F$, [41]. This happens for $\rho = 1/2$ and dimerization, one-third filling and trimerization, and so on. The quasiperiodic model is expected to show this transition, at densities ρ_1 and ρ_2 , because $\alpha = 2k_F$ in these cases. Even for the other commensurate densities ρ_3, ρ_4, \dots , the critical behavior is similar to the periodic potential or Peierls (periodic hopping) case as shown in Ref. [42] although the resonance condition is not strictly valid. In our case, the numerical data obtained for ρ_3 and ρ_4 show the Peierls transition at $V \approx -1.4$ and $\mu \rightarrow 0$ for ρ_3 and at $V \approx -1.5$ and $\mu > 0.1$ for ρ_4 , cf. Fig. 5. Hence, the transition occurs for decreasing particle density at increasing μ . This observation is confirmed by an investigation of the energy spectrum. In the non-interacting case it contains no gap at $\mu = 0$ but $M - 1$ gaps at $\mu = 1$ for the given α [55]. As seen in Ref. [56] most of the gaps open successively for increasing μ . Especially, the first gap at $\alpha/2$ opens for $\mu \rightarrow 0$. Tuning the filling factor, the Fermi points fall into the additional gaps in the spectrum, leading to insulating behavior.

In addition, the behavior seen numerically is in agreement with the weak-coupling RG treatment [42] of spinless fermions on a Fibonacci lattice. The RG equations show the same critical behavior as for the Peierls model, namely

$$\frac{d\mu}{d \ln M} = (2 - K)\mu, \quad (9)$$

where $K = \pi/2 \arccos(-V/2)$ is the Luttinger parameter for half filling. Since the Luttinger parameter does not depend strongly on the filling, it is valid to use this analytical expression for other fillings, too. In accordance with this RG equation we expect, that the phase sensitivity — as in a disordered system [15] — decreases in the localized regime such that

$$M \Delta E \sim e^{-M/\xi} \quad \text{with} \quad \xi^{-1} \sim \mu^{2/(2-K)}, \quad (10)$$

where it is assumed that the localization length ξ is the only relevant length scale. This behavior is clearly found in the numerical data for, e.g., ρ_3 and $V = -0.6$ as shown in Fig. 7. Near the phase transition, it is numerically difficult to distinguish clearly between localized and critical phases. First, for small system sizes and small μ , the decrease in the phase sensitivity is always algebraic, according to the RG equation. Second, the exponential decrease with ξ sets in far from the transition points as shown in Fig. 8. We call this intermediate region, where no universal algebraic or exponential decrease is found, transition region. For ρ_4 , it is difficult to detect and is not separately marked in Fig. 5. There we can only distinguish whether the phase sensitivity decreases or not.

Furthermore, for small $\mu \lesssim 0.2$, the first order phase transition at $V = -2$ remains unaffected. However, for larger μ values, the metallic phase extends towards smaller V values. In comparison to the features of the models with periodic or random distortions, the phase sensitivity shows an unexpected sharp maximum — as already observed in Ref. [31] — for $\mu \gtrsim 0.8$ at $V \lesssim -2$. A similar maximum is also seen for $\mu > 1$ and small system sizes ($M = 34$), nevertheless the system is insulating. The exponential scaling in the localized region as shown in Fig. 7 or Fig. 8 does not change for $V > -2$ and $V < -2$ in the case of large μ . Therefore, we conclude that this regime belongs to the quasiperiodic potential localized regime. On the other hand, no scaling behavior is found for $V < -2$ and small μ (lower left corner in the phase diagram). Here, the localization is due to the formation of particle clusters in the phase-separated state. In the crossover regime between these two localized phases a metallic state is recovered.

VI. CONCLUSIONS

In this work, we have studied and compared the interplay of disorder and interactions for a quantum system at very low (TIP) and finite densities. For TIP, we calculated the pair localization lengths for a quasiperiodic potential and Hubbard interaction by means of the decimation method and obtained the critical parameters from the fit using the one-parameter scaling hypothesis. For non-interacting particles and the onsite interaction we get the value of the critical quasiperiodic potential strength $\mu_c = 1$ and the critical exponent $\nu \approx 1$ in agreement with the results of transfer-matrix-method calculations and finite-size scaling [14]. The results for $U > 1$ show that this conclusion remains valid also for much stronger interactions.

For densities ρ_3 and ρ_4 , we have deduced the phase diagrams of the nearest-neighbor interacting system (7) for varying quasiperiodic potential strength μ and interaction V by the DMRG. The numerically accessible filling factors which are commensurate with the quasiperiodic

potential yield a Peierls-like behavior of the system. The transition at $\mu_c = 1$ is only seen for incommensurate filling or fixed particle number.

In summary, we have studied the influence of interactions on an MIT in a quasiperiodic model in 1D. Our results suggest that the delocalization found previously for low density TIP in the localized phase cannot simply be extrapolated to the finite-density situation. At finite densities, other effects such as a Peierls-like commensurability become important and dominate the transport properties.

ACKNOWLEDGMENTS

We gratefully acknowledge the support of Deutsche Forschungsgemeinschaft within Sonderforschungsbereich 393 (RAR and MS) and 484 (CS). This work was also supported by the SMWK.

[1] B. Kramer and A. MacKinnon, *Rep. Prog. Phys.* **56**, 1469 (1993).

[2] E. Abrahams, P. W. Anderson, D. C. Licciardello, and T. V. Ramakrishnan, *Phys. Rev. Lett.* **42**, 673 (1979).

[3] D. Belitz and T. R. Kirkpatrick, *Rev. Mod. Phys.* **66**, 261 (1994).

[4] S. V. Kravchenko *et al.*, *Phys. Rev. Lett.* **77**, 4938 (1996).

[5] D. Belitz and T. R. Kirkpatrick, *Phys. Rev. B* **58**, 8214 (1998).

[6] D. Simonian, S. V. Kravchenko, M. P. Sarachik, and V. M. Pudalov, *Phys. Rev. Lett.* **79**, 2304 (1997).

[7] D. Simonian, S. V. Kravchenko, M. P. Sarachik, and V. M. Pudalov, *Phys. Rev. B* **57**, R9420 (1998), cond-mat/9712223.

[8] S. V. Kravchenko *et al.*, *Phys. Rev. B* **58**, 3553 (1997), cond-mat/9709255.

[9] V. M. Pudalov, G. Brunthaler, A. Prinz, and G. Bauer, *Pis'ma ZhETF* **65**, 887 (1997), [*JETP Lett.* **65**, 887 (1997)], cond-mat/9707054.

[10] D. L. Shepelyansky, *Phys. Rev. Lett.* **73**, 2607 (1994).

[11] D. L. Shepelyansky, in *Correlated fermions and transport in mesoscopic systems*, edited by T. Martin, G. Montambaux, and J. T. T. Ván (Editions Frontières, Proc. XXXI Moriond Workshop, Gif-sur-Yvette, 1996), p. 201.

[12] R. A. Römer and M. Schreiber, *Phys. Rev. Lett.* **78**, 515 (1997).

[13] D. L. Shepelyansky, *Phys. Rev. B* **54**, 14896 (1996).

[14] A. Eilmes, U. Grimm, R. A. Römer, and M. Schreiber, *Eur. Phys. J. B* **8**, 547 (1999).

[15] P. Schmitteckert *et al.*, *Phys. Rev. Lett.* **80**, 560 (1998).

[16] P. Schmitteckert, R. Jalabert, D. Weinmann, and J.-L. Pichard, *Phys. Rev. Lett.* **81**, 2308 (1998), cond-mat/9804053.

[17] R. A. Römer, M. Schreiber, and T. Vojta, *phys. stat. sol. (b)* **211**, 681 (1999).

[18] R. A. Römer, M. Schreiber, and T. Vojta, accepted by *Physica E* (2000).

[19] M. Leadbeater, R. A. Römer, and M. Schreiber, *Eur. Phys. J. B* **8**, 643 (1999).

[20] R. A. Römer, M. Leadbeater, and M. Schreiber, *Ann. Phys. (Leipzig)* **8**, 675 (1999).

[21] A. MacKinnon and B. Kramer, *Z. Phys. B* **53**, 1 (1983).

[22] K. Frahm, A. Müller-Groeling, J. L. Pichard, and D. Weinmann, *Europhys. Lett.* **31**, 169 (1995).

[23] D. Brinkmann *et al.*, *Eur. Phys. J. B* **10**, 145 (1998).

[24] D. Weinmann, A. Müller-Groeling, J.-L. Pichard, and K. Frahm, *Phys. Rev. Lett.* **75**, 1598 (1995).

[25] F. v. Oppen, T. Wettig, and J. Müller, *Phys. Rev. Lett.* **76**, 491 (1996).

[26] P. H. Song and D. Kim, *Phys. Rev. B* **56**, 12217 (1997).

[27] S. Aubry and G. André, *Ann. Israel Phys. Soc.* **3**, 133 (1980).

[28] A. Barelli, J. Bellisard, P. Jacquod, and D. L. Shepelyansky, *Phys. Rev. Lett.* **77**, 4752 (1996).

[29] A. Barelli, J. Bellisard, P. Jacquod, and D. L. Shepelyansky, *Phys. Rev. B* **55**, 9524 (1997).

[30] P. H. Song and F. v. Oppen, *Phys. Rev. B* **59**, 46 (1999), cond-mat/9806303.

[31] J. C. Chaves and I. I. Satija, *Phys. Rev. B* **55**, 14076 (1997).

[32] C. N. Yang and C. P. Yang, *Phys. Rev.* **150**, 321 (1966).

[33] C. N. Yang and C. P. Yang, *Phys. Rev.* **150**, 327 (1966).

[34] V. E. Korepin, N. M. Bogoliubov, and A. G. Izergin, *Quantum Inverse Scattering Method and Correlation Functions* (Cambridge University Press, New York, 1993).

[35] B. S. Shastry and B. Sutherland, *Phys. Rev. Lett.* **65**, 243 (1990).

[36] B. Sutherland and B. S. Shastry, *Phys. Rev. Lett.* **65**, 1833 (1990).

[37] R. A. Römer and A. Punnoose, *Phys. Rev. B* **52**, 14809 (1995).

[38] S. R. White, *Phys. Rev. Lett.* **69**, 2863 (1993).

[39] S. R. White, *Phys. Rep.* **301**, 187 (1998).

[40] R. Pai, A. Punnoose, and R. A. Römer, preprint SFB 393 97-12, Technische Universität Chemnitz, 1997 (unpublished).

[41] C. Schuster, Ph.D. thesis, (Shaker Verlag, 1999, Aachen).

[42] C. Vidal, D. Mouhanna, and T. Giamarchi, *Phys. Rev. Lett.* **83**, 3908 (1999).

[43] U. Grimm, (1999), Habilitationsschrift, Technische Universität Chemnitz.

[44] C. J. Lambert and D. Weaire, *phys. stat. sol. (b)* **101**, 591 (1980).

[45] D. J. Thouless, *Phys. Rep.* **13**, 93 (1974).

[46] K. Slevin and T. Ohtsuki, *Phys. Rev. Lett.* **82**, 382 (1999), cond-mat/9812065.

[47] F. Milde, R. A. Römer, M. Schreiber, and V. Uski, *Eur. Phys. J. B* **15**, 685 (2000), cond-mat/9911029.

[48] W. H. Press, B. P. Flannery, S. A. Teukolsky, and W. T. Vetterling, *Numerical Recipes in FORTRAN*, 2nd ed. (Cambridge University Press, Cambridge, 1992).

[49] F. D. M. Haldane, *Phys. Rev. Lett.* **47**, 1840 (1981).

[50] W. Kohn, *Phys. Rev.* **133**, A171 (1964).

- [51] D. Loss, Phys. Rev. Lett. **69**, 343 (1992).
- [52] P. Schmitteckert, Ph.D. thesis, Universität Augsburg, 1996.
- [53] R. E. Peierls, *Quantum Theory of Solids* (Oxford University Press, Oxford, 1955).
- [54] W. P. Su, J. P. Schrieffer, and A. J. Heeger, Phys. Rev. B **22**, 2099 (1980).
- [55] A. G. Abanov, J. C. Talstra, and P. B. Wiegman, Phys. Rev. Lett. **81**, 2112 (1998).
- [56] T. Geisel, R. Ketzmerick, and G. Petschel, Phys. Rev. Lett. **66**, 1651 (1991).

TABLE I. Values of the critical quasiperiodic disorder strength μ_c and the critical exponent ν obtained by the non-linear fit for various U values. The first row for each U gives values and the orders n_i , m_i , used in the expansion (4–6), for which the best fits have been obtained. In all cases we find $n_r = 3$ and $m_r = 2$. For μ and M the range of the values which were used in the fit is given. The second row contains values of the critical parameters obtained from a weighted average of fits for various choices of n_i and m_i .

U	μ	M	n_i	m_i	μ_c	ν
0	0.96 – 1.01	55 – 377	2	1	0.989 ± 0.001	1.00 ± 0.15
	0.95 – 1.05	13 – 377	0 – 2	0 – 1	0.99 ± 0.02	1.3 ± 0.5
1	0.97 – 1.05	13 – 377	2	1	0.997 ± 0.001	1.19 ± 0.16
	0.95 – 1.05	13 – 377	0 – 2	0 – 1	0.99 ± 0.01	1.3 ± 0.4
2	0.97 – 1.05	55 – 144	0	0	1.001 ± 0.002	1.14 ± 0.11
	0.95 – 1.05	13 – 144	0 – 2	0 – 1	0.99 ± 0.02	1.5 ± 1
3	0.95 – 1.05	13 – 144	2	1	1.000 ± 0.002	1.16 ± 0.08
	0.95 – 1.05	13 – 144	0 – 2	0 – 1	1.00 ± 0.02	1.8 ± 1
4	0.97 – 1.05	55 – 144	0	0	1.000 ± 0.003	1.12 ± 0.10
	0.95 – 1.05	13 – 144	0 – 2	0 – 1	1.00 ± 0.01	1.5 ± 0.8
5	0.95 – 1.05	13 – 144	1	1	1.002 ± 0.002	1.20 ± 0.09
	0.95 – 1.05	13 – 144	0 – 2	0 – 1	1.00 ± 0.01	1.2 ± 0.3
6	0.95 – 1.05	55 – 144	0	0	0.999 ± 0.002	1.28 ± 0.08
	0.95 – 1.05	13 – 144	0 – 2	0 – 1	1.00 ± 0.02	1.3 ± 0.1
7	0.95 – 1.05	55 – 144	0	0	0.997 ± 0.002	1.28 ± 0.07
	0.95 – 1.05	13 – 144	0 – 2	0 – 1	1.00 ± 0.01	1.5 ± 0.6
8	0.97 – 1.05	55 – 144	0	0	1.001 ± 0.002	1.16 ± 0.08
	0.95 – 1.05	13 – 144	0 – 2	0 – 1	0.99 ± 0.02	1.4 ± 0.4
9	0.97 – 1.05	13 – 144	1	1	1.000 ± 0.001	1.15 ± 0.05
	0.95 – 1.05	13 – 144	0 – 2	0 – 1	1.00 ± 0.01	1.4 ± 0.5
10	0.97 – 1.05	55 – 144	0	0	1.000 ± 0.002	1.23 ± 0.08
	0.95 – 1.05	13 – 144	0 – 2	0 – 1	1.00 ± 0.01	1.4 ± 0.4

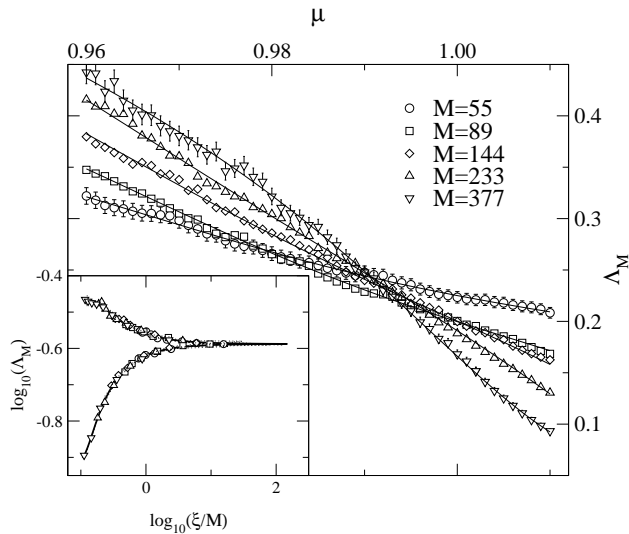


FIG. 1. Reduced localization lengths Λ_M versus quasiperiodic disorder strength μ for $U = 0$. For clarity, only error bars for $M = 55$ and 377 are given. The lines are the fits to the data given by Eq. (3). Inset: Scaling function (thick line) and scaled data points. Only every 4th data point is represented by a symbol for clarity.

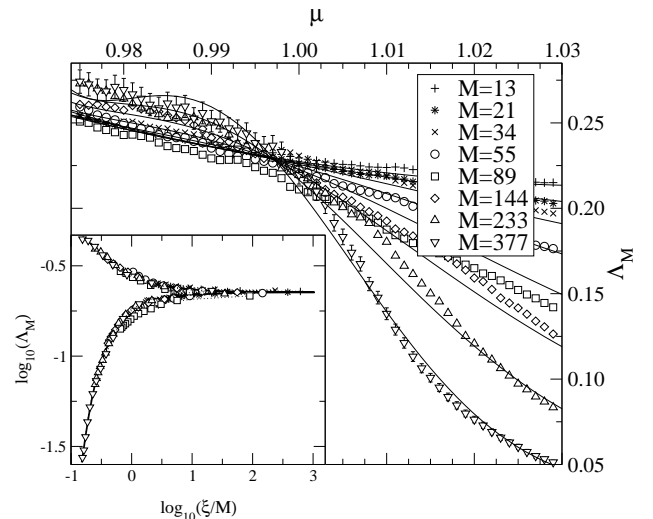


FIG. 2. Reduced localization lengths Λ_M versus quasiperiodic disorder strength μ for $U = 1$. For clarity, only error bars for $M = 377$ are given. The lines are the fits to the data given by Eq. (3). Inset: Scaling function (thick line) and scaled data points. Only every 4th data point is represented by a symbol for clarity.

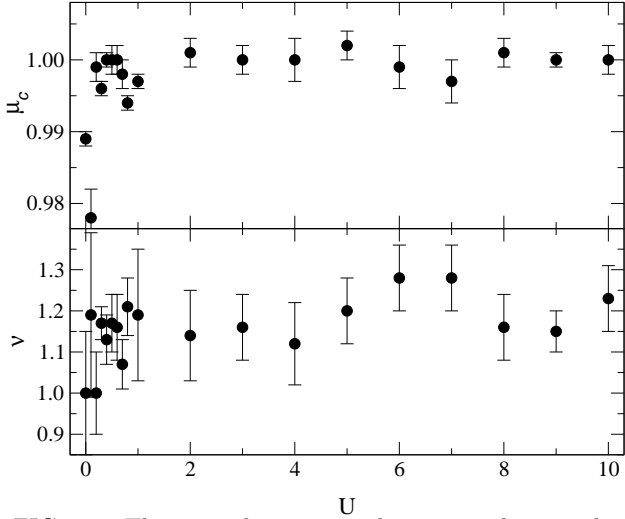


FIG. 3. The critical quasiperiodic potential strength μ_c (upper panel) and the critical exponent ν (lower panel) versus Hubbard interaction strength U . Error bars mark the errors resulting from the Levenberg-Marquardt method of the non-linear fit.

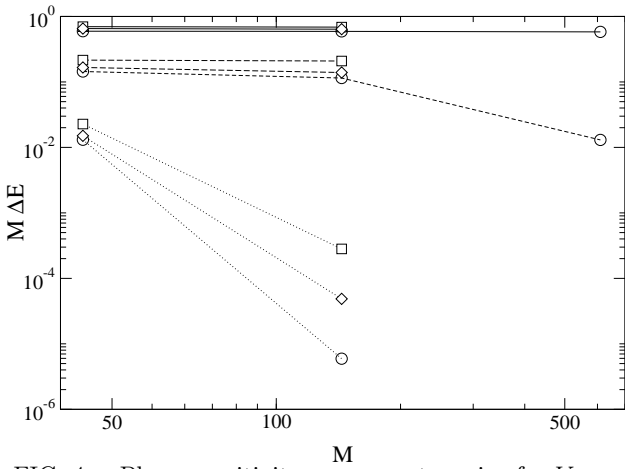


FIG. 4. Phase sensitivity versus system size for $V = -1$ (squares), 0 (circles), 1 (diamonds) at half filling. The three cases $\mu = 0.9$ (solid lines), $\mu = 1$ (dashed lines), and $\mu = 1.1$ (dotted lines) are compared.

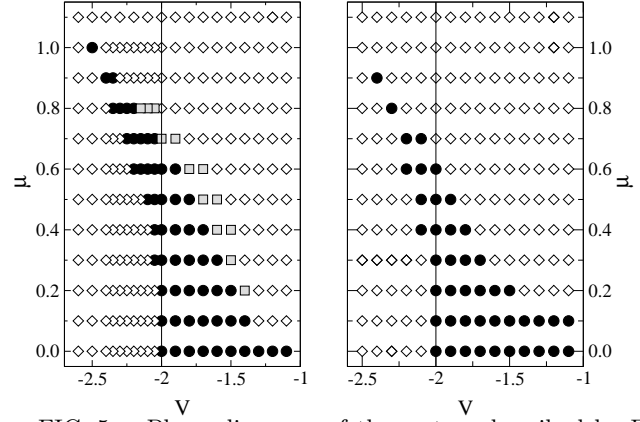


FIG. 5. Phase diagrams of the system described by Eq. (7) in terms of quasiperiodic potential strength μ and the interaction V for $\rho = \rho_3$ (left side) and $\rho = \rho_4$ (right side). An extended ground state wave function is marked by \bullet , a localized by \diamond . In addition, the transition regime (see text) is marked with a shaded \square in the left figure. The solid lines indicate the first-order transition at $V = -2$.

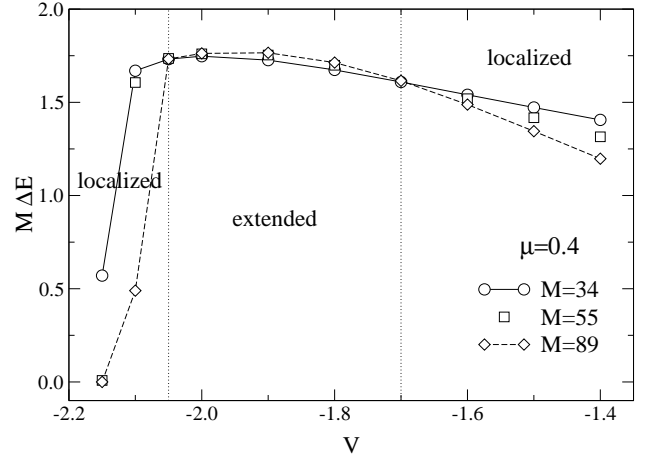


FIG. 6. Phase sensitivity versus interaction for three different system sizes, density ρ_3 and $\mu = 0.4$. The lines for $M = 34$ and 89 are guides to the eye, highlighting the different finite-size-scaling behaviors in the various regimes. The dotted lines indicate the transition between the localized and the extended wave functions.

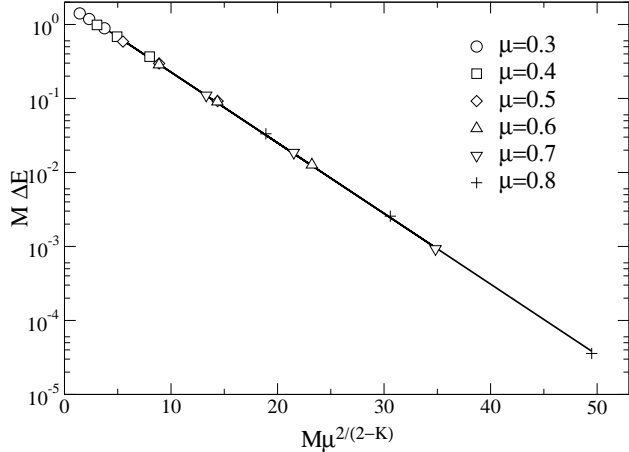


FIG. 7. Phase sensitivity versus scaled system size $M\mu^{2/(2-K)}$, where $M = 34, 55$, and 89 , for $V = -0.6$, filling $\rho = \rho_3$, and various potential strengths. The line indicates a plot of Eq. (10) with $K = \pi/2 \arccos(0.3) \approx 1.24$.

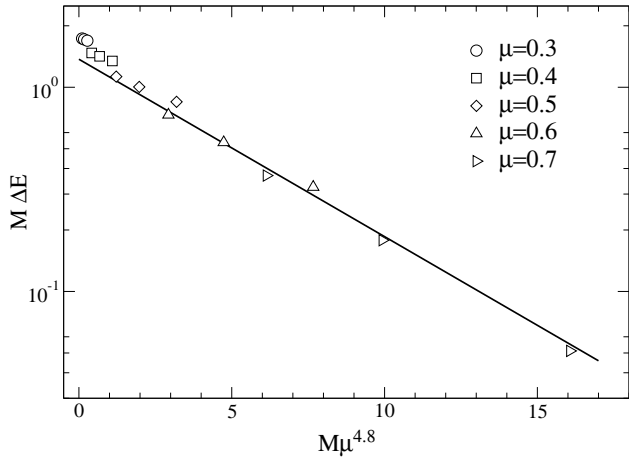


FIG. 8. Phase sensitivity versus scaled system size, $M = 34, 55$, and 89 , for $V = -1.5$ and ρ_3 . The straight line is a fit to the data for $\mu = 0.7$ and 0.8 .